International Journal of Astrophysics and Space Science
2025; 13(2): 21-35
http://www.sciencepublishinggroup.com/j/ijass
doi: 10.11648/j.ijass.20251302.11
ISSN: 2376-7014 (Print); ISSN: 2376-7022 (Online)

Variation of Total Electron Content over May 10 - 13 2024 Geomagnetic Super Storm in South Africa

Efrem Amanuel Data*

Department of Physics, College of Natural and Computational Science, Wolaita Sodo University, Wolaita Sodo, Ethiopia

Email address:
immanuelefawu@gmail.com

To cite this article:
Efrem Amanuel Data. (2025). Variation of Total Electron Content over May 10 - 13 2024 Geomagnetic Super Storm in South Africa. *International Journal of Astrophysics and Space Science, 13*(2), 21-35. https://doi.org/10.11648/j.ijass.20251302.11

Received: 4 March 2025; **Accepted:** 27 March 2025; **Published:** 11 April 2025

Abstract: This study investigates the variation of Total Electron Content (TEC) over South Africa during the geomagnetic superstorm of May 10 - 13, 2024. This study aims to analyze the variation of TEC over South Africa during the May 10 - 13, 2024, geomagnetic superstorm using data from the IRI-2020 model, GNSS-based TEC measurements, and other geomagnetic parameters. The root mean square error (RMSE) method was applied to quantify the deviations between GPS-derived TEC measurements and the IRI-2020 model during the geomagnetic storm. The results reveal significant TEC fluctuations, with a pronounced increase during the main phase due to prompt penetration electric fields (PPEFs) and storm-induced ionospheric disturbances. This was followed by a sharp TEC depletion in the recovery phase, attributed to thermospheric composition changes, particularly oxygen-to-nitrogen ratio variations. Magnetometer H-component observations further confirm the strong geomagnetic activity associated with the storm, indicating enhanced ionospheric currents and electrodynamic coupling. Latitudinal variations in TEC revealed complex ionospheric dynamics, with more pronounced disturbances at mid-latitudes. The ionospheric irregularities affected GNSS-based positioning, highlighting the impact of geomagnetic storms on navigation systems. These findings provide valuable insights into ionospheric storm effects over South Africa, contributing to improved space weather forecasting, GNSS accuracy, and regional ionospheric modeling.

Keywords: Super Storm, Mid-latitude Ionosphere, PPEFs, TEC, Storm-time

1. Introduction

The Earth's ionosphere, a region of the upper atmosphere consisting of ionized particles. Its density, often quantified by the TEC, is highly dynamic, responding to solar and geomagnetic forcing [2]. Geomagnetic storms are significant disturbances in the Earth's magnetosphere caused by solar wind and interplanetary magnetic field interactions. These storms can have profound effects on the ionosphere, which is a important parameter for understanding ionospheric behavior and its impact on communication and navigation systems [14]. It was a fast and energetic coronal mass ejection (CME) ejected from an active sunspot region on the Sun. CMEs are large eruptions of plasma and magnetic fields that are expelled from the Sun's corona at speeds ranging from 300 km/s to over 3,000 km/s. It associated with this storm was likely Earth-directed, meaning it traveled directly toward our planet and X-class solar flare, which represents the most intense category of solar flares [1]. The CME reached Earth within 15–24 hours of the initial eruption, indicating it was moving at an extremely high velocity (>2,000 km/s). The Interplanetary Magnetic Field (IMF) carried by the CME had a strong southward B_z component, which allowed efficient energy transfer into Earth's magnetosphere [4]. Once the CME impacted Earth, it caused a rapid and severe geomagnetic disturbance. The interaction between the CME's magnetic field and Earth's magnetosphere triggered a significant geomagnetic response, leading to major disruptions in Earth's space environment. The storm's effects were amplified by high solar wind speeds (over 800 km/s) and strong southward IMF orientation [3]. The geomagnetic superstorm that occurred from May 10 to 13, 2024, was one of the most intense events recorded in recent years [15, 10, 26]. The disturbance caused massive energy injections into the Van Allen radiation belts, enhancing the risk to satellites and astronauts. The Disturbance Storm Time

(Dst) index, a key measure of geomagnetic storm intensity, likely dropped below -200 nT, which is indicative of a very strong storm. The Dst index represents the global decrease in Earth's horizontal magnetic field strength, caused by an intensified ring current around the planet [5]. A value below -200 nT is classified as a superstorm, in comparison, the famous Carrington Event in 1859 had an estimated Dst of about -850 nT, while the Halloween Storms 2003 reached around -400 nT [2]. Superstorm was the appearance of spectacular auroras at unusual latitudes. Auroras, normally confined to Polar Regions, were seen in mid-latitude. The extreme geomagnetic conditions allowed for red, green, and purple aurora displays, caused by oxygen and nitrogen interactions in the ionosphere. Such aurora activity indicates major energy deposition into the upper atmosphere, which also leads to ionospheric disturbances [6]. The ionosphere is severely affected by the superstorm and the TEC is a measure of free electrons in the ionosphere, and its fluctuations affect GNSS/GPS signal accuracy. The strongest impacts were seen in mid-latitude regions like South Africa, where radio signals experienced increased absorption and signal degradation [7].

Previous studies have shown that geomagnetic storms can cause significant enhancements or depletions in TEC, depending on various factors such as, latitude, and the intensity of the storm. The prompt penetration electric field (PPEF) and disturbance dynamo electric field (DDEF) are two primary mechanisms that influence TEC variations during geomagnetic storms [5-7, 16]. However, there are no studies analyzing superstorm-driven ionospheric disturbances over South Africa. This study aims to fill the scientific gap regarding the impact of extreme space weather events on South Africa's ionosphere and technological systems. It seeks to provide empirical data on TEC variations, and GNSS errors during superstorms. Also, it will contribute to the development of space weather monitoring and mitigation strategies for South Africa and the broader mid-latitude region.

2. Data and Methodology

2.1. Ionospheric TEC Data Sources

2.1.1. GNNS/GPS TEC Data

GNSS/GPS TEC variation at superstorm event data downloaded from the NSF GAGE Data Server is a platform provided by the National Science Foundation (NSF) that supports the Geophysical and Atmospheric Research (GAGE) program. (https://gage-data.earthscope.org/archive/gnss/rinex/obs). The RINEX file calliborated by using Gopi Seemala software 3.5 version.

2.1.2. IRI-2020 Model TEC Data

The TEC data for the South African sector using the IRI-2020 model is typically obtained through the International Reference Ionosphere (IRI) model, which provides global ionospheric parameters, including TEC, based on different input parameters [8]. The IRI-2020 model is the latest version of the model and more accurate predictions are offered by it. The IRI model (2020 version) is made available through the official website by the International Union of Radio Science (URSI) and the Ionospheric and Space Weather Research Center. TEC data can be requested by users based on the geographical region, time, and solar conditions, with the longitude and latitude bounds for the sector being defined at https://iri.gsfc.nasa.gov/ and access to ionospheric data and predictions, including TEC data based on the IRI model, is provided by SWDN https://swindon.nasa.gov/.

2.2. Geomagnetic Indices and Solar Activity Data

Planetary Geomagnetic Index (Kp index) is a global scale used to measure the magnitude of geomagnetic disturbances caused by solar activity, such as solar wind and solar flares. It provides a summary of geomagnetic activity at various locations on Earth.

Disturbance Storm Time Index (Dst index) is a measure of the intensity of geomagnetic storms based on variations in the Earth's magnetic field. It quantifies the strength of the ring current, a system of charged particles that encircle the Earth in the equatorial plane of the magnetosphere.

Auroral Electrojet Index (AE) - Also from WDC Kyoto. IMF and Solar Wind Data - NASA OMNIWeb (https://omniweb.gsfc.nasa.gov/).

2.3. Magnetometer Data

Magnetometer data is available from numerous local and global sources. Ground-based magnetometer stations provide geomagnetic field readings at one-second, one-minute, and one-hour intervals. The data is available from INTERMAGNET (https://www.intermagnet.org/). To access and download the data navigated to the data section of the INTERMAGNET website. The time resolution of one minute, which is suitable for this study, and specify the date range corresponding to the super storm periods.

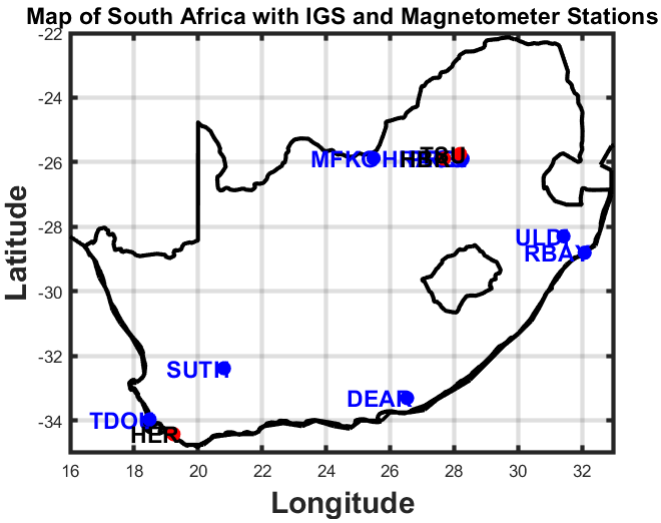

Figure 1. *Study area map for South African region.*

Table 1. *Geographic locations of South African IGS and Magnetometer stations.*

Station Code	Station Name	Latitude (∘N)	Longitude (∘E)	Elevation (m)
HRAO	Hartebeesthoek (HRAO)	-25.8897	27.6854	1415
SUTH	Sutherland (SUTH)	-32.3800	20.8100	1798
RBAY	Richards Bay (RBAY)	-28.8020	32.0835	53
PRE3	Pretoria (PRE3)	-25.8895	28.2683	1385
PRE4	Pretoria (PRE4)	-25.8895	28.2683	1385
SBOK	Springbok (SBOK)	-29.6693	17.8792	1043
DEAR	De Aar (DEAR)	-33.3026	26.5324	746
MFKG	Mafikeng (MFKG)	-25.8761	25.4861	1143
ULDI	Ulundi (ULDI)	-28.2939	31.4231	607.9
TDOU	Tdou (TDOU)	-33.9642	18.4847	630.2

Table 2. *True geographic locations of South African Magnetometer stations.*

Station Code	Station Name	Latitude (∘N)	Longitude (∘E)
HBK	Hartebeesthoek Magnetometer (HBK)	-25.8897	27.6854
TSU	Tshwane (TSU)	-25.7460	28.1880
HER	Hermanus (HER)	-34.4195	19.2331

2.4. Thermospheric O/N_2 Ratio Data

The thermospheric O/N_2 ratio refers to the ratio of atomic oxygen (O) to molecular nitrogen (N_2) in the thermosphere, the upper layer of Earth's atmosphere. This ratio is an important parameter in space weather and ionospheric studies because it influences ionospheric electron densities. It is primarily derived from satellite-based ultraviolet (UV) observations. The main sources of O/N_2 data for this study from Global Ultraviolet Imager (GUVI) on the TIMED satellite Provides daily O/N_2 maps using far-ultraviolet (FUV) emissions. https//guvitimed.jhuapl.edu/home_guvi-datausage Diurnal variations are higher during the day due to solar heating and photo dissociation, and lower at night due to decreased temperatures and recombination. Geomagnetic storm effects Storm-driven upwelling increases N_2, reducing O/N_2, leading to ionospheric depletion. These space weather conditions can impact the performance of GPS and communication satellites, leading to potential disruptions in ionosphere. Therefore, continuous monitoring and understanding of O/N_2 variations are essential for maintaining reliable space-based technologies. Data gaps are limited spatial and temporal coverage from satellite instruments. To address these gaps, a combination of ground-based observations and advanced modeling techniques can be employed.

2.5. Quiet-Day Reference

For a precise assessment of the TEC variability during quiet days on May 07-09, 2024, over South Africa, choosing suitable quiet-day references is essential. May 7 and 9, 2024 According to related studies, these days are geomagnetically quiet and occur just before the storm commencement. For example, studies examining the ionospheric reaction to the storm in May 2024 used May 7 and 9 as reference days, which were quiet and showed no disturbed geomagnetic activity. A quiet-day reference TEC was created using average TEC values from May 9-10, 2024, during quiet geomagnetic conditions (Kp $\leq$ 3) in order to identify storm impacts and (Dst $\leq$ -20) [14].

2.6. TEC Calculation

Slant TEC (STEC) was computed from GNSS observations using code and carrier phase measurements. Vertical TEC (VTEC) was then derived by mapping STEC values to the vertical using a standard mapping function [25]. In order to precisely extract electronic content from dual-frequency GNSS data, the International GNSS Service (IGS) offers high-quality products. A important step in this process is addressing differential code biases (DCBs) found in both satellite and receiver measurements. These biases, if left uncorrected, can introduce significant errors in the calculation of the slant Total Electron Content (sTEC). To mitigate this, IGS DCB products are meticulously applied as corrections to the measured pseudo-range and carrier phase data. The sTEC itself is then derived from a combination of these corrected pseudo-range and carrier phase measurements collected at two distinct frequencies, commonly denoted as f_1 and f_2. This combination is specifically designed to isolate the ionospheric delay, thereby providing a reliable estimate of the electronic content along the signal path.

$$\text{sTEC} = \frac{\Delta\Phi}{K} \tag{1}$$

where:

1. $\Delta\Phi = \lambda_1\Phi_1 - \lambda_2\Phi_2$ is the difference in carrier phases (Φ_1, Φ_2) at wavelengths λ_1, λ_2.
2. $K = \frac{f_1^2 f_2^2}{f_1^2 - f_2^2} \times 40.3$, a constant relating frequency and

TECU.
3. $f_1 = 1575.42$ MHz
4. $f_2 = 1227.60$ MHz

The relation between sTEC and vTEC is given by:

$$\text{vTEC} = \text{sTEC} \times \cos(\zeta) \tag{2}$$

where:

$$\cos(\zeta) = \sqrt{1 - \left(\frac{R_e \cos E}{R_e + h}\right)^2} \tag{3}$$

with:
1. ζ Zenith angle of the signal path.
2. R_e Earth's radius.
3. h Effective ionospheric height.
4. E Elevation angle of the satellite.

Substituting sTEC and obliquity factor $F(E)$

$$\text{vTEC} = \frac{\Delta\Phi}{K} \times \left[1 - \left(\frac{R_e \cos E}{R_e + h}\right)^2\right]^{1/2} \tag{4}$$

2.7. Statistical Metrics

The Root Mean Square Error (RMSE) is used to evaluate the accuracy of GPS-derived TEC compared to the IRI-2020 model. The RMSE is defined as

$$\text{RMSE} = \sqrt{\frac{1}{N}\sum_{i=1}^{N}\left(TEC_{\text{GPS}} - TEC_{\text{IRI-2020}}\right)^2}$$

where TEC_{GPS} is the observed TEC from GPS receivers. $TEC_{\text{IRI-2020},i}$ is the modeled TEC from the IRI-2020 model. N is the total number of observations. The RMSE provides a quantitative measure of the deviation between the GPS-derived TEC and the IRI-2020 model predictions.

3. Results

The result focuses on diurnal TEC variation at all south African stations, at storm season, during quiet time, the solar wind parameters, SYM-H, thermospheric O/N_2, magnetometer and lastly the TEC value performance between IRI - 2020 and GNSS/GPS ionospheric TEC data result respectively. Pre-storm is noticeable increase in TEC was observed during initial storm hours. Main Phase is TEC peaked in the afternoon and evening, with deviations from quiet-day values. Spatial Variations is non-uniform TEC enhancements were observed across different stations. Depletion Phase in TEC depletion occurred after the main phase. Recovery Phase in TEC gradually returned to normal levels by May 13. Correlation Analysis is a strong negative correlation was found between Dst and TEC, indicating ring current influence. The differences observed between May 10 and 13 indicate the following storm effects Positive Storm Phase (May 10–11) Enhanced TEC levels suggest increased ionization due to storm-driven energy input, possibly from Joule heating and electric field penetration. Negative Storm Phase (May 12–13) The reduction in TEC on May 12 indicates possible ionospheric depletion due to changes in neutral composition, particularly enhanced molecular nitrogen, leading to increased recombination rates. Model Performance The IRI-2020 model consistently overestimates TEC during disturbed conditions, highlighting the need for model adjustments to accommodate extreme storm effects. The Figure 3 shows how the TEC changed during the geomagnetic superstorm of May 10–13, 2024 at five different locations in the South African sector DEAR, RBAY, TDOU, ULDI, and HRAO. The IRI-2020 model is represented by the red curves, and the observed GPS-TEC is represented by the blue curves. The ionospheric reaction to the geomagnetic disturbance is indicated by the notable differences between the modeled and observed TEC. Understanding and forecasting ionospheric behavior, which can affect satellite communication and navigation systems, requires accurate TEC modeling. Differences between TEC as observed and as modeled can be used to identify weaknesses in existing models and direct enhancements. Furthermore, reducing the impact of space weather on technology infrastructure requires accurate TEC models. The observed GPS-TEC data provides valuable insights into the actual ionospheric conditions during geomagnetic disturbances, which can be compared to the IRI-2020 model predictions. This comparison allows researchers to assess the model's performance and identify areas where it may need improvement, particularly in capturing the complex dynamics of the ionosphere during space weather events. By refining and enhancing TEC models based on these comparisons. Figure 3 also illustrates the TEC variations at multiple stations (i.e. DEAR, RBAY, TDOU, ULDI, and HRAO) over four consecutive days. The key observations are as follows

3.1. Day-to-Day TEC Variability

May 10, 2024 TEC values exhibit a significant enhancement during the daytime, with peak TEC reaching approximately 50 TECU. The IRI-2020 model (red line) overestimates TEC during peak hours but aligns well during the nighttime. The GPS-TEC (blue line) shows a wavelike structure, suggesting increased ionospheric irregularities.

May 11, 2024 Compared to May 10, TEC values remain high but show a slightly earlier peak, indicating a shift in ionospheric response. The discrepancy between the model and observed TEC is more pronounced, especially in the post-sunset period, suggesting storm-induced disturbances.

May 12, 2024 A clear suppression of TEC is observed relative to the previous days, especially during the peak hours. This suggests a depletion of ionospheric plasma, likely due to storm-time electrodynamics, including the penetration of electric fields and changes in thermospheric composition.

May 13, 2024 TEC values begin to recover but remain lower than May 10 and 11, particularly during the daytime. The night-time TEC is relatively stable, indicating a gradual return to pre-storm conditions. The IRI-2020 model continues

to overestimate TEC, highlighting the storm's impact on ionospheric predictions.

Figure 2 to differentiate the TEC variations for each IGS station in quiet time, (May 07-09) and storm-time (May 10-13) behavior separately for each station ULDI, TDOU, PRE3, PRE4, HRAO, and DEAR. The quiet-time data provides a baseline for normal TEC behavior at each station. The storm-time data reveals how different IGS stations respond uniquely to geomagnetic storms. The differences in TEC patterns among stations highlight the complexity of ionospheric storm effects across South Africa. During geomagnetically quiet conditions; TEC exhibits a predictable diurnal pattern, primarily driven by solar radiation. Typically, TEC increases throughout the day and peaks at local noon as a result of strong solar ionization. Declines at night, as recombination processes dominate in the absence of solar radiation. Maintains stable trends, with smooth variations across different stations (ULDI, TDOU, PRE3, PRE4, HRAO, DEAR). The Disturbance Storm Time (Dst) index remains relatively stable, indicating no significant geomagnetic disturbances.

3.2. Station-wise TEC Behavior During Quiet vs. Storm Periods

ULDI & TDOU More affected by positive storm effects, with TEC increases due to plasma redistribution. PRE3 & PRE4 Show negative storm effects, likely due to storm-driven winds pushing ionized particles to lower altitudes. HRAO Exhibits strong storm-induced TEC variability, possibly due to its geomagnetic location. DEAR Displays the highest degree of perturbations, indicating extreme storm-induced ionospheric irregularities.

3.3. Interpretation of Each Station's TEC Response

Stations closer to the magnetic equator (e.g., PRE3, PRE4) are more likely to experience negative storm effects due to the strong equatorial electric field disturbances. Stations at mid-latitudes (e.g., HRAO, DEAR) experience both enhancements and depletions, driven by traveling ionospheric disturbances (TIDs). Storm-time electrodynamics caused different TEC effects at each station, depending on Geomagnetic latitude The time during storm onset Influence of storm-driven electric fields and winds The May 10-13 storm caused strong disturbances in the ionosphere, significantly altering TEC levels. The Dst index likely showed deep negative values, indicating severe geomagnetic activity. The storm-time TEC variability could have affected GPS positioning, satellite communications, and HF radio signals due to ionospheric irregularities. The presence of positive and negative storm effects across different regions suggests that storm-induced electric fields and neutral winds played a major role in TEC redistribution. The quiet-time dataset serves as a reference to understand normal TEC variations before storm impacts. The storm-time dataset highlights extreme deviations, demonstrating how ionospheric storms disrupt normal TEC behavior. Further analysis (numerical or modeling-based) can quantify storm-time deviations and help refine ionospheric prediction models for the African sector.

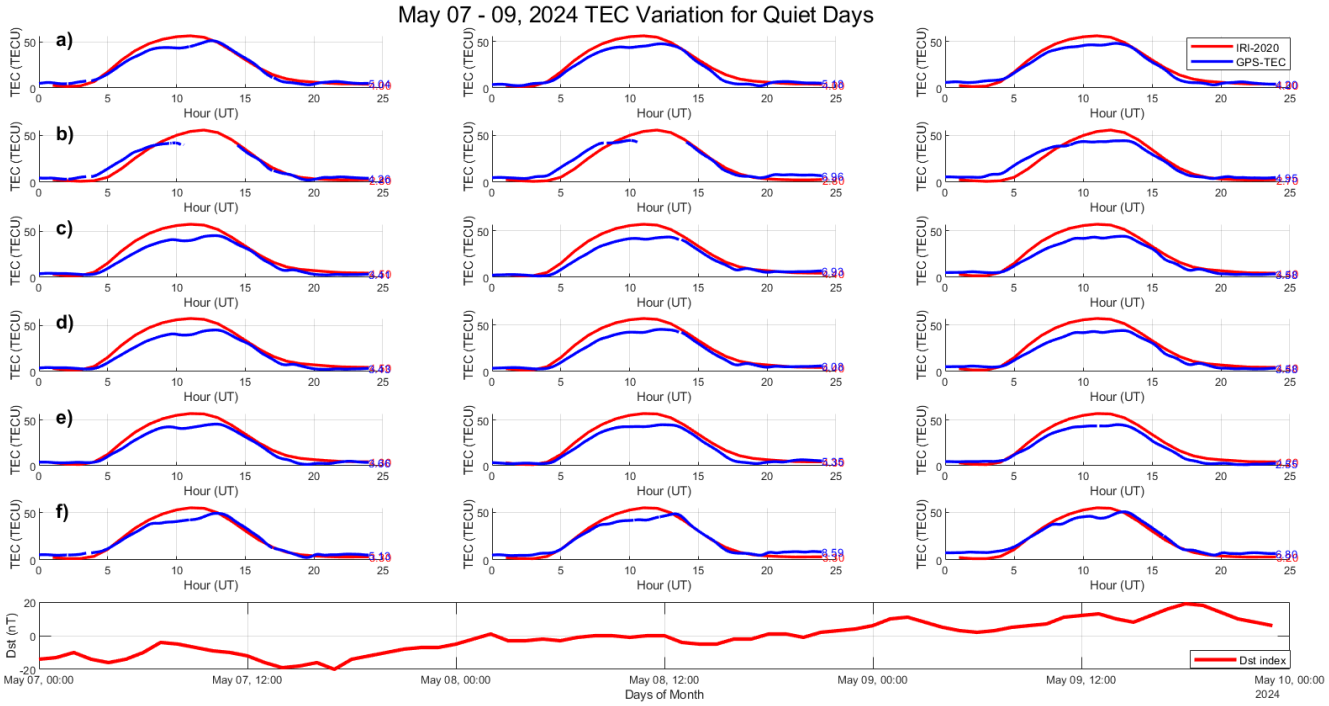

Figure 2. Panel a) for ULDI station, panel b) for TDOU station, panel c) for PRE3 station, panel d) for PRE4 station, e) for HRAO station, and panel f) for DEAR station TEC variations during quiet time reference with disturbance storm time (Dst) index in May 07 - 09 2024.

The Figure 2 variation of TEC over the period of May 07 - 09, 2024, during the quiet time in South Africa, the provided Root Mean Square Error (RMSE) values for the South African IGS stations (ULDI, TDOU, PRE3, PRE4, HRAO, DEAR) from the dataset you provided.

Review of RMSE Data

The RMSE values given correspond to different stations for three specific quiet time points `Doy 128`, `Doy 129`, and `Doy 130`. The RMSE values for each station across the three quiet time periods

Table 3. *Root Mean Square Error values for different stations over days of the year (doy) 128, 129, and 130.*

Station	RMSE for doy		
	128	**129**	**130**
ULDI	4.9199	5.3331	4.6859
TDOU	4.1739	5.1953	6.2556
PRE3	7.8643	7.8269	7.1084
PRE4	7.9731	6.9931	7.1559
HRAO	6.6429	6.5506	6.5565
DEAR	5.0282	5.0826	4.7000

The RMSE values for quiet time represent the discrepancy between the observed and predicted TEC values. Lower RMSE values suggest better model performance in predicting TEC, while higher values indicate greater deviation. ULDI station shows a slight increase in RMSE from `Doy 128` (4.92) to `Doy 129` (5.33), followed by a decrease in `Doy 130` (4.69). TDOU station shows a significant increase in RMSE from `Doy 128` (4.17) to `Doy 129` (5.20), and then a further increase to 6.26 in `Doy 130`. PRE3 and PRE4 show variations, with PRE4 having a noticeable drop in RMSE between `Doy 128` (7.97) and `Doy 129` (6.99), but both remain high. HRAO shows minimal variation in RMSE across the three datasets, hovering around 6.55. DEAR has relatively stable RMSE values across all time periods.

A spike in RMSE values (especially at stations like TDOU) may indicate higher variability or inaccuracies in TEC measurements during geomagnetic activity. Lower RMSE values in stations like ULDI and DEAR suggest more stable or better predictions, likely due to lower disturbances in the ionosphere. The trend of RMSE changes could reflect different responses to the geomagnetic storm on May 07 - 09, 2024. For example, stations with increasing RMSE values may experience greater ionospheric disturbance or noise during the geomagnetic storm. The increased RMSE in certain stations (e.g., TDOU, PRE4) suggests that the storm had a varying impact on different regions. The RMSE might have increased due to disturbances in the ionosphere, leading to greater discrepancies in TEC measurements. This could be an indication of ionospheric irregularities such as TEC depletions, enhancements, or fluctuations caused by the geomagnetic storm. The storm's effect is more prominent at certain stations like TDOU, where RMSE increases, indicating larger discrepancies in TEC. Stations like ULDI and DEAR show more stable measurements, suggesting that their TEC predictions might have been less influenced by the storm or they are better modeled.

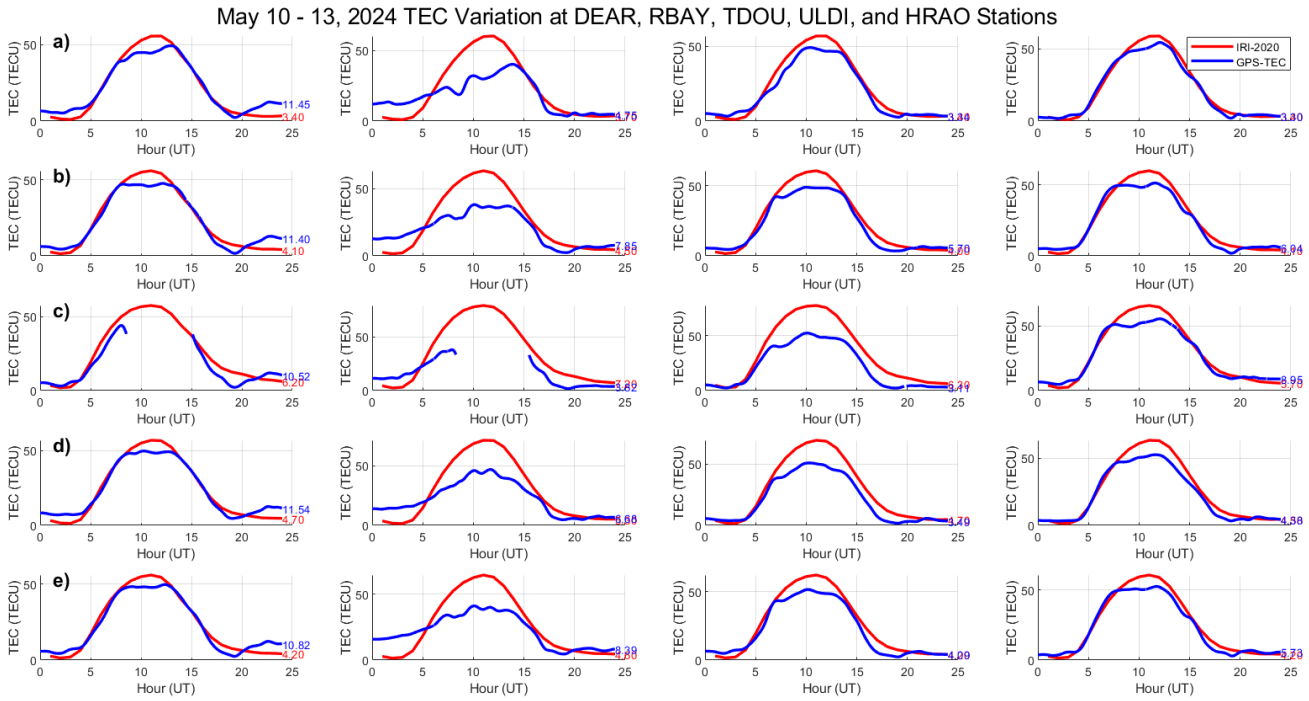

Figure 3. *Panel a) for DEAR station, panel b) for RBAY station, panel c) for TDOU station, panel d) for ULDI station, and e) for HRAO station TEC variations from many sides in South Africa at super storm time in May 10 - 13 2024.*

This Figure (4) presents the TEC variation recorded at five South African stations (SUTH, PRE3, PRE4, SBOK, and MFKG) during the geomagnetic superstorm event from May 10 - 13, 2024. The GPS-derived TEC is compared with the IRI-2020 model-predicted TEC, providing insight into how the storm-induced ionospheric disturbances deviated from climatological expectations.

The GPS-TEC exhibits significant deviations from the IRI-2020 model, particularly during the daytime hours (07:00 - 16:00 UT), indicate storm-induced ionospheric disturbances. The most pronounced TEC enhancement is observed around midday across all stations, with peak TEC values exceeding the expected IRI values by up to 10 - 20 TECU, suggesting an abnormal increase in ionospheric electron density. The enhancement is likely due to increased energy input from the storm, which drives strong electrodynamic processes such as storm-time ionospheric uplift and changes in plasma transport.

TEC Depletion during the Recovery Phase

Post-sunset after 18:00 UT, a sharp decline in TEC is observed at most stations, falling below the IRI-2020 model predictions. This indicates storm-induced ionospheric depletion, possibly due to Enhanced recombination processes reducing electron density. changes in neutral composition brought on by storms, especially a rise in molecular species (N2, O2) that may result in electron loss. Plasma redistribution on a large scale as a result of disturbance and penetration into electric fields.

IRI-2020 Model Underestimation of Storm-Time Effects The IRI-2020 model fails to capture the strong enhancements and subsequent depletions during the storm. This suggests that empirical models like IRI, which are based on long-term climatology, do not account for short-term storm-time dynamics affecting TEC. This underestimation highlights the importance of using real-time GPS-TEC measurements for space weather monitoring and forecasting, particularly during geomagnetic disturbances.

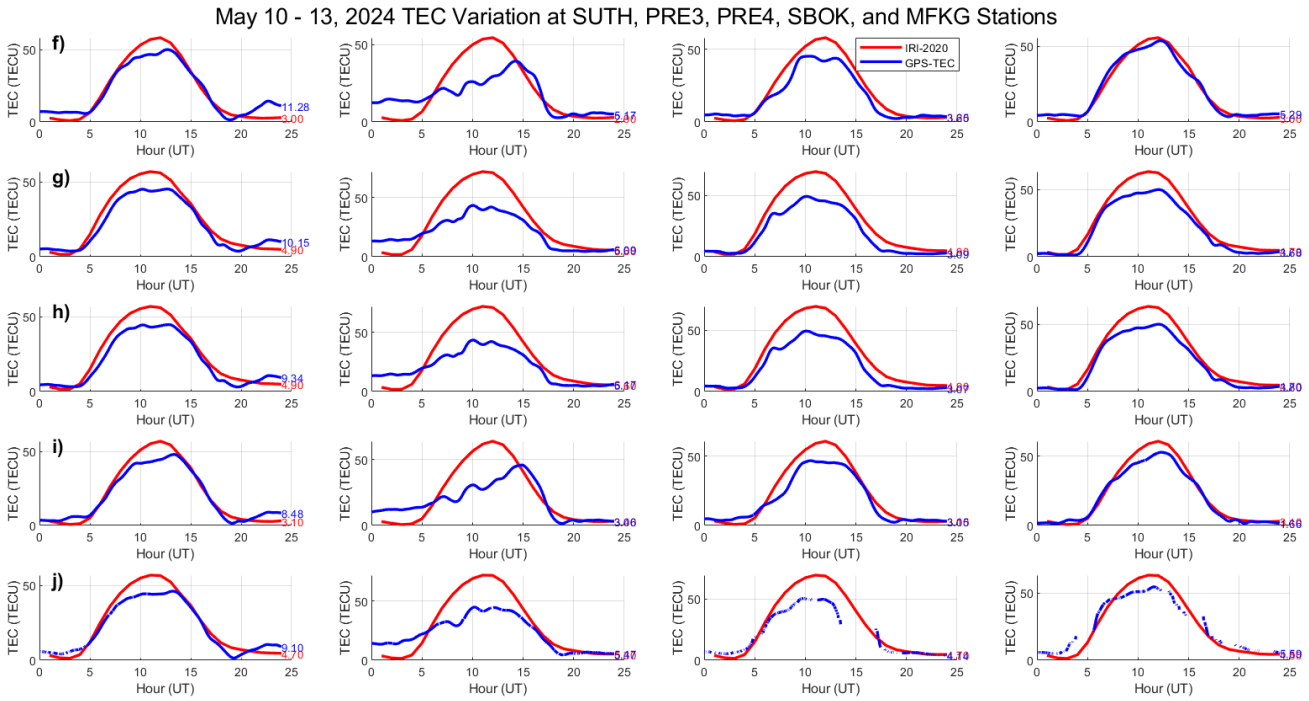

Figure 4. *Panel f) for SUTH station, panel g) for PRE3 station, panel h) for PRE4 station, panel i) for SBOK station, and panel j) for MFKG station TEC variations from many sides in South Africa at super storm time in 2024.*

3.4. Storm-Time Ionospheric Response

A significant increase in TEC observed between 10 and 15 Universal Time (UT) suggests ionospheric disturbances linked to geomagnetic storm activity. Geomagnetic storms, triggered by solar events such as coronal mass ejections (CMEs) or solar flares, cause substantial perturbations in the Earth's magnetosphere and ionosphere [13]. These disturbances can lead to enhanced ionization and changes in electron density distribution, resulting in TEC variations. The observed increase in TEC during this time frame is likely due to the injection of energetic particles into the upper atmosphere and subsequent ionization processes. Such storm-time ionospheric responses can have significant implications for satellite communications, GPS accuracy, and other technological systems that rely on radio wave propagation through the ionosphere. The under prediction of TEC at specific stations during storm events indicates that the model does not fully capture the rapid and localized enhancements caused by storm-driven electric fields and thermospheric disturbances. The IRI-2020 model's limitations stem from The absence of real-time storm effects such as PPEFs and rapid plasma redistribution. Incomplete depiction of the neutral

composition variations brought on by storms. the use of empirical data that would not accurately reflect extremely dynamic or extreme ionospheric circumstances. Incorporating real-time satellite and ground-based measurements could help improve the model's accuracy during storm events. Utilizing data from GNSS networks and ionosondes can provide timely insights into ionospheric changes. Additionally, integrating space weather monitoring tools could enhance the model's ability to predict rapid and localized disturbances [9]. Post-storm effects, such as TEC depletion and nighttime irregularities, are visible across the stations, suggesting storm-driven plasma redistribution. The findings demonstrate how intricate relationships among electric fields, thermospheric dynamics, and geomagnetic storms influence notable changes in ionospheric TEC. The underestimating of peak TEC values during storm circumstances by the IRI-2020 model indicates the need for better modeling methods that take real-time storm characteristics into account. With consequences for space weather monitoring and GNSS applications, post-storm impacts such as TEC depletion and abnormalities at night highlight the long-term effects of geomagnetic disturbances on the ionosphere.

3.5. Regional Differences in TEC Disturbances

The stations exhibit varying TEC magnitudes, which could be attributed to geomagnetic latitude, local electrodynamics, and storm-time penetration electric fields [11]. Geomagnetic latitude influences the distribution of charged particles in the ionosphere, affecting the TEC. Regions at higher geomagnetic latitudes often experience more significant TEC variations due to increased interactions with the Earth's magnetic field. These interactions can enhance ionospheric irregularities, leading to fluctuations in TEC levels. The strongest TEC deviations are recorded at TDOU station, indicating a more pronounced storm impact in this region. This could be due to its geographical location, which may be more susceptible to geomagnetic disturbances. Also, local factors such as unique atmospheric conditions or proximity to auroral zones might amplify the effects of storm-time electric fields. Consequently, these elements contribute to the more significant TEC deviations observed at TDOU station.

3.6. The May 2024 Superstorm

The geomagnetic storm on May 10–13, 2024, also referred to as the "Mother's Storm Day", was one of the most intense space weather events in recent years. It was driven by a sequence of fast coronal mass ejections (CMEs) from the Sun, leading to sustained geomagnetic disturbances (Dst $\leq$ -250 nT) [12]. Similar ionospheric disturbances were reported globally, with enhanced equatorial ionization anomalies (EIAs) and storm-time electric field penetration affecting satellite-based navigation and communication systems [10]. The observed TEC deviations from the IRI-2020 model confirm the strong impact of the May 2024 superstorm on the ionosphere over the South African sector. This study highlights the importance of real-time monitoring and improved modeling for space weather prediction and mitigation of ionospheric disturbances.

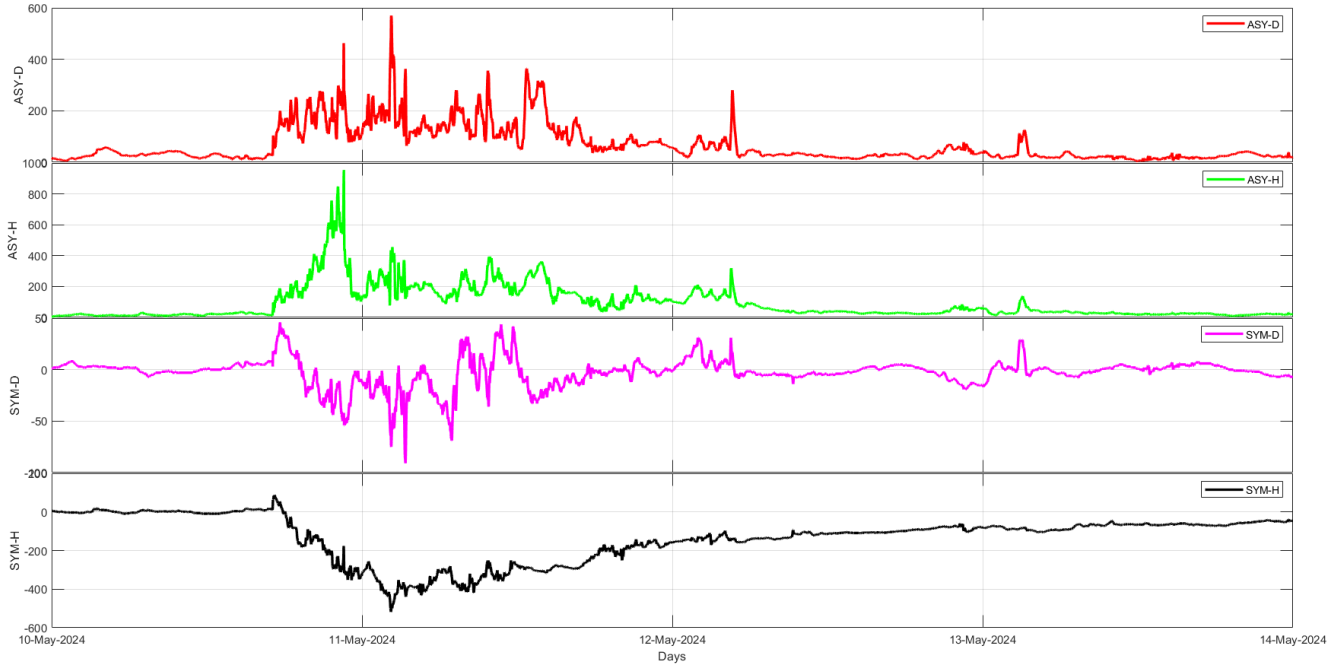

Figure 5. *Solar wind parameters Bz GSE/GSM, Kp index, Dst index and AE/AL index values time in UT days from May 10 to May 13, 2024.*

The four indices in figure 5 provide insights into the geomagnetic activity ASY-D (Red) represents the asymmetric disturbance in the horizontal geomagnetic field. A significant increase is observed on May 11, suggesting enhanced magnetospheric convection. ASY-H (Green) displays a sharp peak on May 11, indicating intense aurora and ring current activity. SYM-D (Magenta) reflects storm-time disturbances, with fluctuations indicating sub storm activity. SYM-H (Black) Shows a major depression below -200 nT, confirming a strong geomagnetic storm, possibly linked to an interplanetary coronal mass ejection (ICME).

3.7. Impact on TEC Variation

During this storm, significant TEC variations were observed over the East African region, likely due to ionospheric disturbances caused by the enhanced energy input into the Earth's upper atmosphere. The geomagnetic storm may have caused Sudden increases in TEC due to ionospheric uplift caused by storm-induced electric fields. Increased recombination rates are probably the cause of TEC depletions in the post-midnight region. Irregularities in the ionosphere, leading to GPS signal scintillation and potential navigation errors.

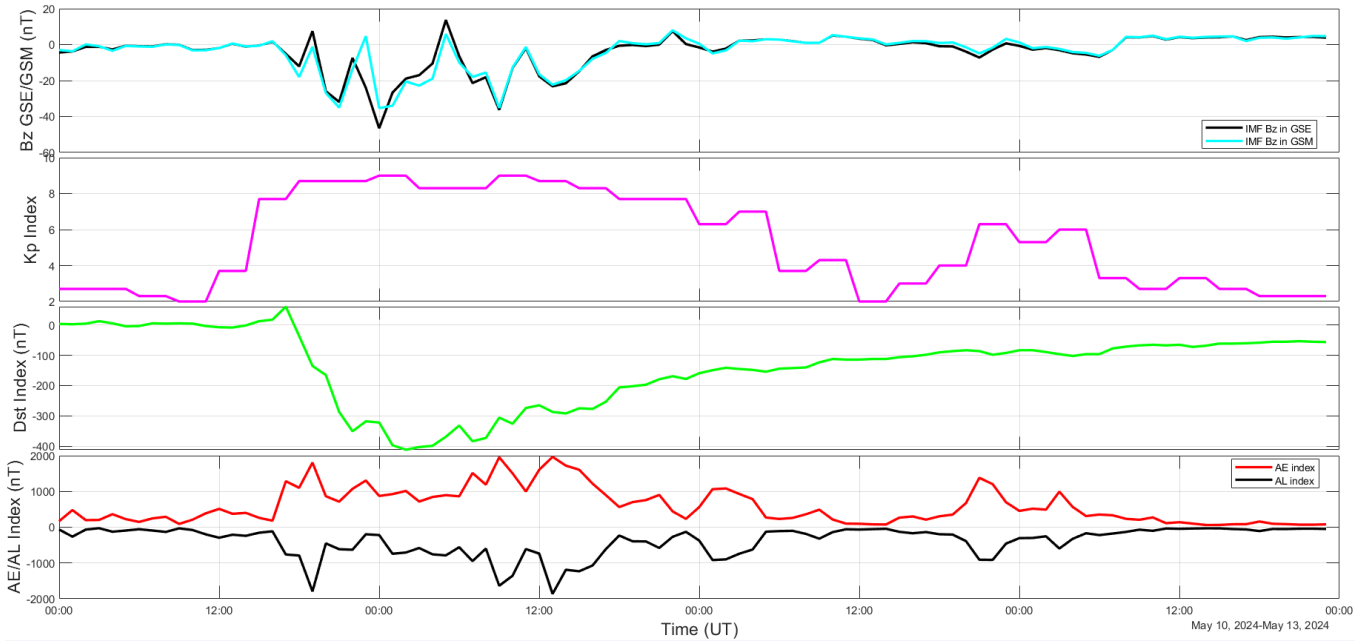

Figure 6. *Solar wind parameters Bz GSE/GSM, Kp index, Dst index and AE/AL index values time in UT days from May 10 to May 13, 2024.*

The Figure (6) presents key space weather parameters during the superstorm event from May 10–13, 2024, over South Africa. Below is an interpretation of each parameter's impact on TEC variability.

IMF Bz (GSE/GSM) (Top Panel) The Interplanetary Magnetic Field (IMF) Bz component (black and cyan lines) shows significant southward excursions (negative values) around May 10–11. A strong negative IMF Bz leads to enhanced geomagnetic activity by facilitating magnetic reconnection at the dayside magnetopause. This triggers increased energy input into the ionosphere, which can cause TEC enhancements or depletions depending on the storm phase.

Kp Index (Second Panel) The planetary Kp index, which measures geomagnetic disturbance, reached values above 8 during the main phase of the storm. A high Kp index indicates strong geomagnetic activity, leading to ionospheric disturbances such as TEC fluctuations, increased ionospheric currents, and possible disruptions in satellite communication and navigation systems over South Africa.

Dst Index (Third Panel) The Disturbance Storm Time (Dst) index, a measure of the ring current strength, dropped significantly below -300 nT, indicating a severe geomagnetic storm. This large negative Dst value suggests strong magnetospheric convection, which can cause ionospheric disturbances, including TEC variations due to changes in electron density distributions.

AE/AL Index (Bottom Panel) The AE index (red) and AL index (black) represent auroral electro jet activity, which indicates magnetospheric sub storm activity. The highly fluctuating AE/AL indices during the storm reflect enhanced auroral currents, which could contribute to ionospheric irregularities and TEC variability due to increased energy deposition in the polar and sub auroral regions. The storm's impact on the ionosphere would include TEC enhancements due to storm-induced ionization, followed by possible TEC depletions due to ionospheric disturbances and electrodynamic effects. The super storm of May 10-13, 2024, caused significant geomagnetic disturbances, as reflected in the SYM-H index dropping below -200 nT.

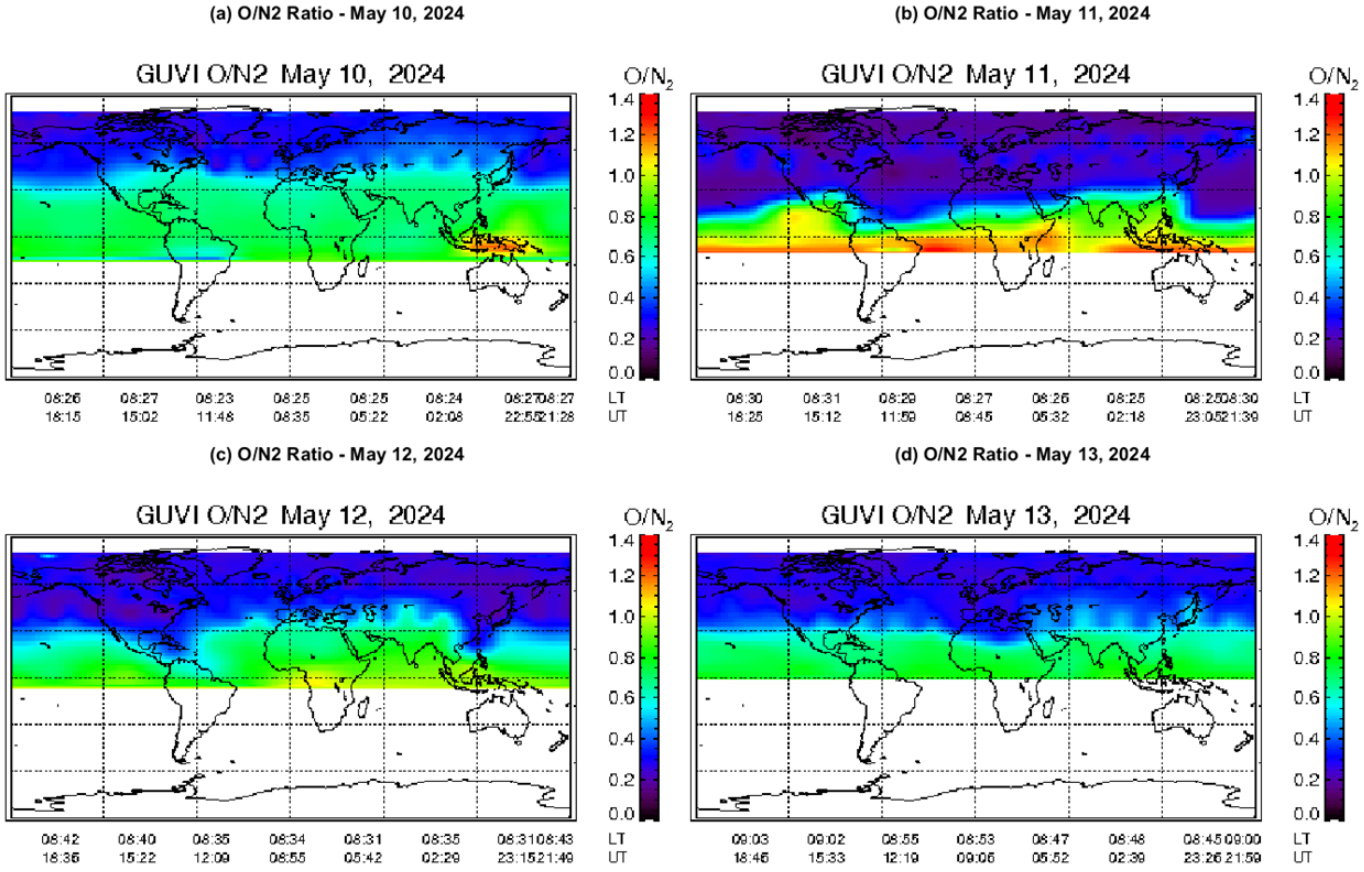

Figure 7. *Global thermospheric $[O]/[N_2]$ map for the period of May 10 - 13, 2024, from the Global Ultraviolet Imager (GUVI) experiment fown on the TIMED satellite. The white spaces in each panel indicate data gaps.*

3.8. O/N_2 over South Africa Region

The Figure (7) show the GUVI instrument's Oxygen-to-Nitrogen (O/N_2) ratio for May 10-13, 2024. One important measure of variations in thermospheric composition, which are greatly impacted by geomagnetic storms, is the O/N_2 ratio. The interpretation for mid-latitudes and the South African region is here.

May 10-11, 2024 An elevated O/N_2 ratio (0.8 - 1.2) was observed over mid-latitudes, suggesting an increase in atomic oxygen. This indicates a potential rise in the concentration of atomic oxygen, which could have implications for atmospheric chemistry and climate models. Further analysis is required to understand the underlying causes and long-term effects of this observation. Storm-driven upwelling pushes molecular nitrogen (N_2) downward, keeping atomic oxygen levels high. This phenomenon could alter ozone formation and depletion rates, impacting air quality and climate dynamics. Understanding these changes is crucial for refining predictive models and developing effective mitigation strategies. Enhanced ionospheric TEC likely caused disruptions in GNSS accuracy and radio communication. These disruptions could affect navigation systems, communication networks, and other technologies reliant on precise positioning and timing. Further research is needed to quantify the extent of these disruptions and develop strategies to mitigate their impact on critical infrastructure.

May 12-13, 2024 A decline in O/N_2 indicated the storm's weakening phase. This was followed by a significant drop in NO_2 levels, suggesting a further decrease in the storm's intensity. By the end of May 13, the storm had dissipated, marking the end of its impact on the region. Increased molecular nitrogen upwelling suppresses ionization, reducing electron density. This reduction in electron density led to a stabilization of the ionosphere, indicating the storm's complete dissipation and the region's return to normal atmospheric conditions. As the storm dissipated, the ionosphere stabilized, leading to a decrease in HF radio communication disturbances and satellite drag effects. The region returned to normal atmospheric conditions, marking the end of the storm's impact.

3.9. Comparison with Other Regions Thermospheric O/N_2 Ratio

In *equatorial regions*, variations in O/N_2 were moderate due to neutral wind dynamics and the equatorial fountain effect. These variations were primarily driven by the interplay between upward and downward winds, which cause a redistribution of oxygen and nitrogen in the atmosphere. The equatorial fountain effect, in particular, plays a significant role by lifting ions and neutrals to higher altitudes, thereby influencing the composition of the upper atmosphere.

In *higher latitudes*, a significant reduction in O/N_2 was observed, likely due to auroral heating and enhanced Joule heating effects. This reduction is attributed to the increased energy input from auroral activity, which heats the thermosphere and alters the distribution of atmospheric gases. Consequently, the higher latitudes experience a distinct atmospheric composition compared to equatorial regions. The peak storm phase (May 10-11) led to enhanced ionization and increased TEC, impacting satellite navigation and radio communication.

3.10. Magnetometer Result

Each station recorded geomagnetic field variations using 1-minute resolution data, capturing critical storm phases including the main phase, sub storm activity, and the recovery phase. The super storm geomagnetic storm that struck the Earth from May 10 to 13, 2024 had a major impact on the magnetosphere. The event was recorded by three south African magnetometer stations HER (Hermanus), TSU Tshwane, and HBK (Hartebeesthoek).

TSU (Tshwane) The Figure (8) H-component drops sharply (450 nT) at the same time as HER (19:00 UTC, May 10). The D-component exhibits strong fluctuations, suggesting increased field-aligned currents. The Z-component follows a similar trend to HER, with a sharp decrease followed by oscillations. The S-component fluctuates noticeably, showing signs of increased ionospheric disturbances.

HBK (Hartebeesthoek) The Figure (9) H-component experiences a rapid drop (400 nT) at 19:00 UTC on May 10. The D-component shows strong fluctuations, indicating interactions with IMF variations. The Z-component reveals strong oscillations, pointing to sub storm effects. The S-component displays increased disturbances, reflecting storm-related geomagnetic perturbations.

HER (Hermanus) The Figure (10) H-component exhibits a sharp decrease (500 nT) around May 10, 19:00 UTC, marking the storm's main phase. The D-component fluctuates significantly during the storm, indicating strong variations in the ionospheric currents. The Z-component shows a rapid decrease followed by irregular fluctuations. The S-component exhibits strong variations, reflecting perturbations in the overall geomagnetic intensity.

Table 4. *Comparison of geomagnetic variations at HER, TSU, and HBK during the May 2024 super storm.*

Station	H (nT)	D-component	Z-component	Impact
HER	500	High fluctuations	Decrease with oscillations	Significant
TSU	450	Moderate fluctuations	Similar to HER	Strong
HBK	400	Noticeable fluctuations	Large oscillations	Strong

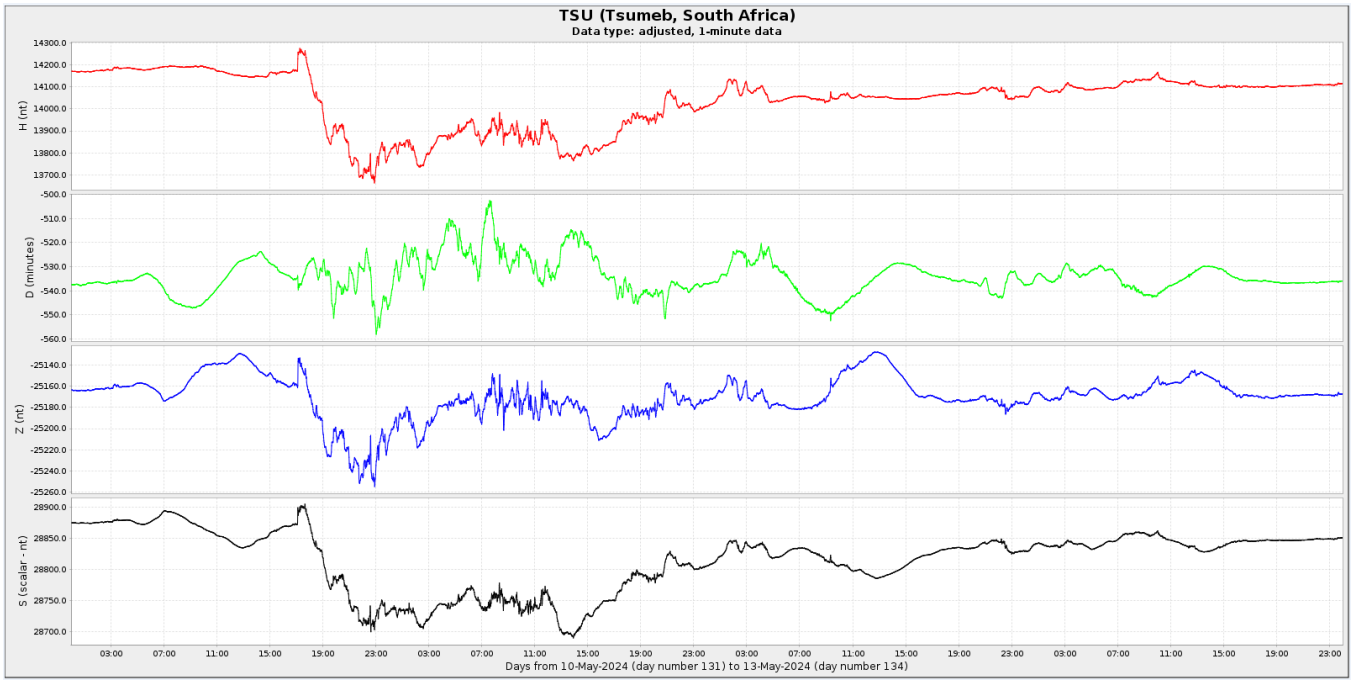

Figure 8. *Magnetometer parameters H, D, Z and Scalar values with time in 10/05/2024 - 13/05/2024 in days of year from 131 - 134 for Tsumeb, south African station.*

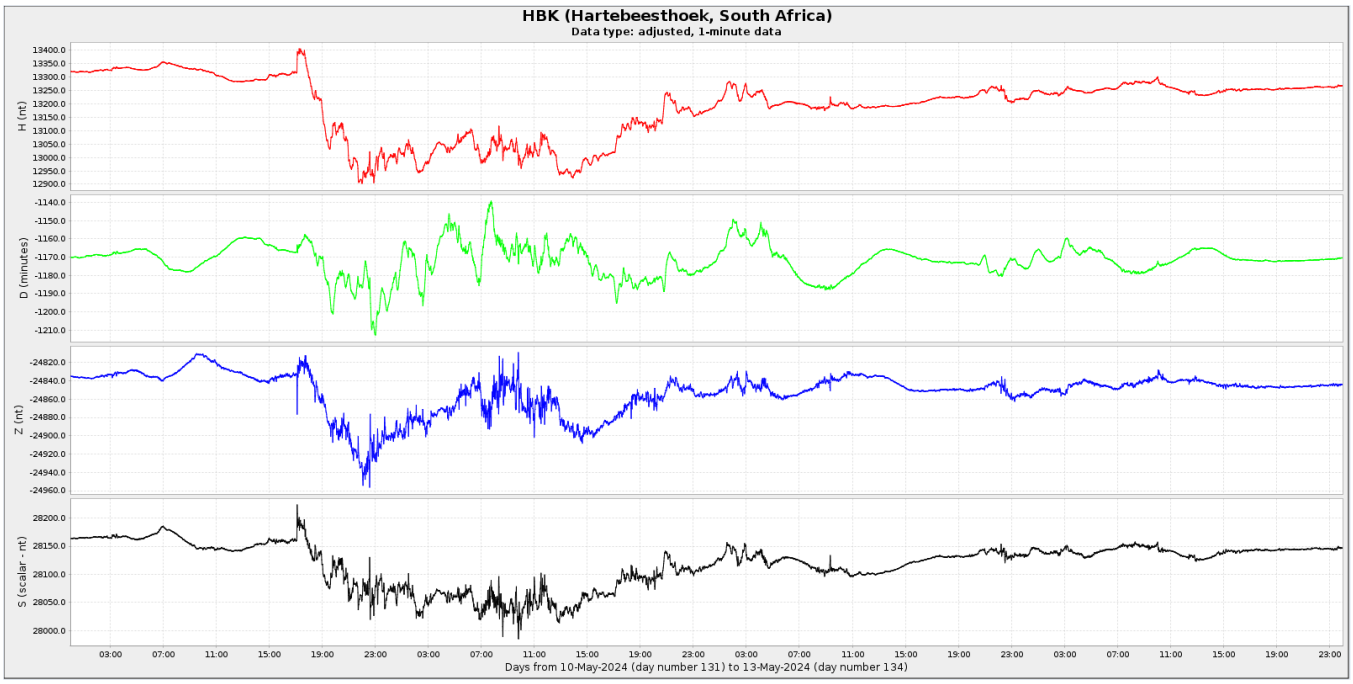

Figure 9. *Magnetometer parameters H, D, Z and Scalar values with time in 10/05/2024 - 13/05/2024 in days of year from 131 - 134 for Hartebeesthoek, south African station.*

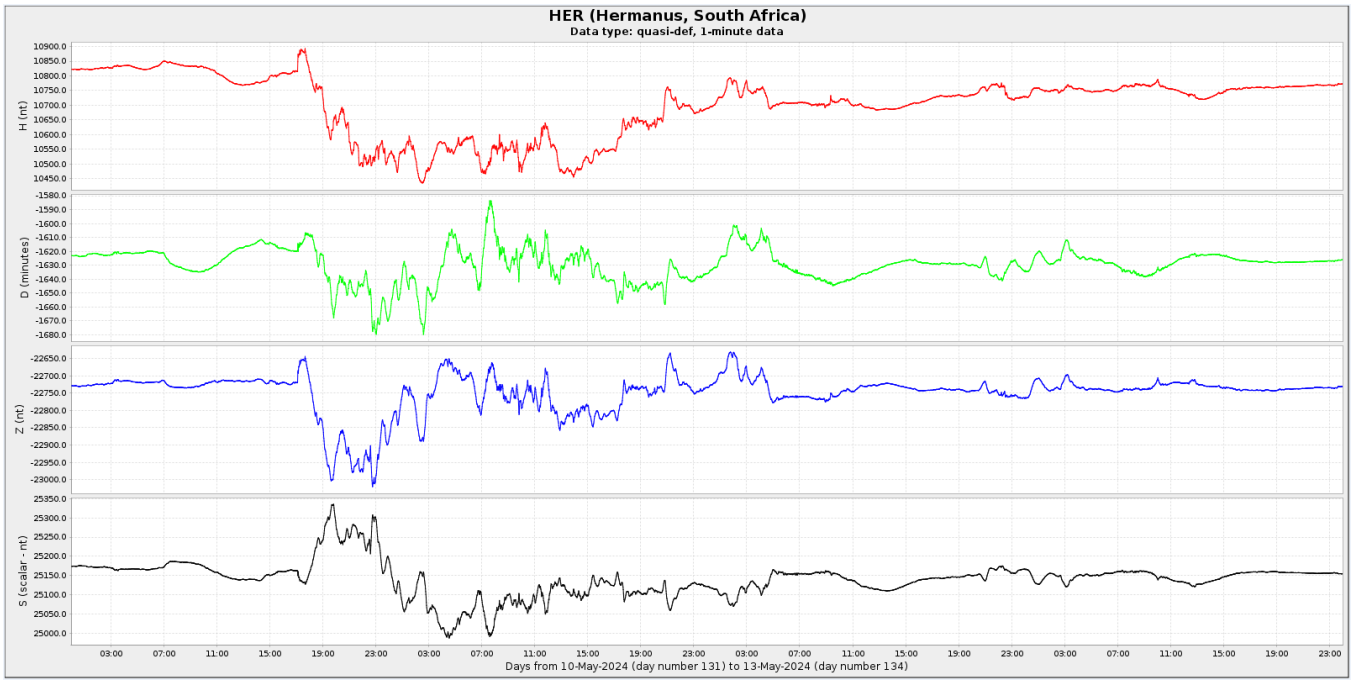

Figure 10. *Magnetometer parameters H, D, Z and Scalar values with time in 10/05/2024 - 13/05/2024 in days of year from 131 - 134 for Hermanus, south African station.*

The super storm of May 10–13, 2024 caused significant geomagnetic disturbances over Africa. The synchronized drop in H, Z, and D components confirms a major ring current enhancement and strong magnetospheric-ionospheric coupling.

4. Discussion

The analysis of TEC variations over South Africa during the geomagnetic superstorm from May 10 - 13, 2024, provides important insights into the ionospheric response to extreme space weather conditions. The observed TEC enhancements and depletions, along with magnetometer disturbances, highlight the storm's impact on ionospheric

dynamics, driven by storm-induced electrodynamics and plasma redistribution.

4.1. Day-to-Day Variability in TEC

On May 10, TEC values exhibited a significant enhancement, with peak TEC reaching approximately 50 TECU during daytime hours. This increase aligns with previous studies that have documented similar storm-time TEC enhancements due to enhanced ionization from energy injection into the ionosphere [17, 18]. The discrepancy between IRI-2020 modeled TEC and observed GPS-TEC values suggests that empirical models may not fully capture storm-time ionospheric dynamics, particularly at low- and mid-latitudes [19]. By May 11, the TEC values remained high but showed a shift in peak occurrence. This temporal shift could be attributed to storm-driven thermospheric composition changes, particularly increases in molecular nitrogen (N_2) and oxygen (O_2), leading to a recombination-induced reduction in plasma density [24]. The sustained TEC enhancements during the post-sunset period further indicate the presence of storm-enhanced density (SED) structures [21]. On May 12, a suppression of TEC was observed, particularly during peak hours, indicating negative storm effects. Such TEC depletions are often associated with storm-time thermospheric cooling and composition changes that reduce ionization efficiency [23]. By May 13, TEC values gradually returned to quiet-time levels, marking the end of the storm's influence on the ionosphere.

Storm-Time Magnetospheric and Ionospheric Coupling The synchronized drop in the H, D, and Z components of the magnetometer data from multiple South African stations indicates a strong enhancement in ring current activity, confirming the coupling between geomagnetic disturbances and ionospheric responses. Previous studies have shown that intense geomagnetic storms enhance ring currents, leading to significant reductions in geomagnetic field components [14]. The observed correlation between TEC variations and magnetometer disturbances suggests that magnetosphere-ionosphere coupling played a key role in the ionospheric perturbations observed during the storm period. Stations such as ULDI and TDOU experienced greater TEC enhancements, likely due to plasma redistribution caused by penetration electric fields (PEFs) and disturbance dynamo effects [20]. In contrast, stations such as PRE3 and PRE4 exhibited negative storm effects, possibly due to storm-driven meridional winds transporting ionized particles to lower altitudes, where recombination rates are higher [17]. The presence of strong TEC variability at HRAO suggests enhanced storm-time traveling ionospheric disturbances (TIDs), a phenomenon commonly observed during strong geomagnetic storms [22].

4.2. Model Performance and TEC Prediction Challenges

The comparison between observed GPS-TEC and IRI-2020 model predictions indicates that the empirical model underestimated storm-induced TEC variations. Similar underestimations have been reported in previous studies, where models fail to capture the full extent of storm-time electrodynamics and composition changes [17,20]. The discrepancies between modeled and observed TEC suggest the need for model refinements, incorporating real-time storm-driven forcing mechanisms to improve forecasting accuracy.

5. Conclusion

This study analyzed the ionospheric response to the May 10 - 13, 2024, geomagnetic superstorm over South Africa using GPS-TEC observations, magnetometer data, and thermospheric composition variations. The key findings indicate:

1. A significant TEC enhancement on May 10 - 11, attributed to storm-driven ionization and electric field penetration.
2. A TEC suppression phase on May 12 - 13, linked to thermospheric composition changes and increased molecular species leading to recombination.
3. Strong magnetosphere-ionosphere coupling evidenced by synchronized geomagnetic disturbances and TEC variations.
4. Spatial variability in TEC response across South African stations, with some locations experiencing positive storm effects (ULD and TDOU) and others showing negative storm effects (PRE3 and PRE4).
5. Limitations in the IRI - 2020 model in predicting storm-induced TEC changes, emphasizing the need for improved modeling approaches.

The results highlight the importance of real-time ionospheric monitoring for understanding space weather effects, particularly in south African region.

Abbreviations

CME	Coronal Mass Ejection
DOY	Day of Year
EIA	Equatorial Ionization Anomaly
GNSS	Global Navigation Satellite System
GPS	Global Positioning System
HF	High Frequency
IMF	Interplanetary Magnetic Field
IRI	International Reference Ionosphere
KP	Planetary Kp Index
PPEFs	Prompt Penetration Electric Fields
RINEX	Receiver-Independent Exchange
RMSE	Root Mean Square Error
sTEC	Slant Total Electron Content
TECU	Total Electron Content Unit
UV	Ultraviolet
vTEC	Vertical Total Electron Content

ORCID

0009-0006-3668-5445 (Efrem Amanuel Data)

Acknowledgments

I would like to express my sincere gratitude to the Global UltraViolet Imager (GUVI) map data for providing valuable ionospheric data. Special thanks to NASA for making their datasets available for scientific research. Appreciation is also extended to the Kyoto Data Center for supplying geomagnetic and space weather data. I am grateful to Dr. Gopi Seemala for developing and providing the GPS-TEC analysis software, which was instrumental in processing and analyzing GNSS data. Acknowledgment is also given to the GAGE (GNSS Analysis and Geodetic Experiment) data source for providing high-quality GNSS/GPS data. Sincere appreciation is extended to the anonymous reviewers for their insightful comments and suggestions, which helped improve the quality of this work.

Author Contributions

Efrem Amanuel Data is the sole author. The author read and approved the final manuscript.

Data Availability Statement

Data can be made available on request.

Funding

This work did not receive any funding.

Conflicts of Interest

The author declare no conflicts of interest.

References

[1] Buzulukova, N. (2017). Extreme events in geospace: Origins, Predictability, and Consequences. Elsevier.

[2] Knipp, D., Hapgood, M., O'brien, T. P., Welling, D., Yue, X., Luk, M., Green, J., Likar, J., & Shprits, Y. (2017). Space Weather Quarterly Volume 14, Issue 3, 2017. Space Weather Quarterly, 14(3), 1'32. https://doi.org/10.1002/swq.15

[3] Kataoka, R. (2022b). Extreme space weather. Elsevier.

[4] Terefe, D. A., Nigussie, M., & Habarulema, J. B. (2024). The effect of energy deposition hemispherical asymmetry on characteristics of LSTIDs during 17 March 2015 geomagnetic storm. Journal of Geophysical Research: Space Physics, 129(5), https://doi.org/10.1029/2023JA031907

[5] Miyake, F., & Poluianov, S. (2019). Extreme solar particle storms: The Hostile Sun. Programme: Aas-Iop Astronomy.

[6] Licata, R. J. (2022). Probabilistic space weather modeling and forecasting for the challenge of orbital drag in space traffic management. https://doi.org/10.33915/etd.11600

[7] Alfonsi, L., Bergeot, N., Cilliers, P. J., De Franceschi, G., Baddeley, L., Correia, E., Di Mauro, D., Enell, C., Engebretson, M., Ghoddousi-Fard, R., Häggström, I., Ham, Y., Heygster, G., Jee, G., Kero, A., Kosch, M., Kwon, H., Lee, C., Lotz, S.,... Zou, S. (2022). Review of environmental monitoring by means of radio waves in the polar regions: from atmosphere to geospace. Surveys in Geophysics, 43(6), 1609-1698. https://doi.org/10.1007/s10712-022-09734-z

[8] Anderson, D. (1999). The Ionosphere.

[9] Bilitza, D., Brown, S., & Reinisch, B. (2022). *IRI-2020: The latest version of the International Reference Ionosphere model*. Advances in Space Research, 70(2), 325–337.

[10] Danilov, A. D., 2013. Ionospheric F-region response to geomagnetic disturRbances. Advances in Space Research, 52(3), pp. 343-366. https://doi.org/10.1016/j.asr.2013.04.019

[11] Correlations between space weather parameters during intense geomagnetic storms: Analytical study. https://doi.org/10.1016/j.asr.2023.07.053

[12] NOAA (2024). *Space Weather Bulletin: Analysis of the May 2024 Geomagnetic Storm*. National Oceanic and Atmospheric Administration, June 2024.

[13] Owens, M. J., Lockwood, M., Barnard, L. A. et al. Extreme Space-Weather Events and the Solar Cycle. Sol Phys 296, 82 (2021). https://doi.org/10.1007/s11207-021-01831-3

[14] Atabati, A., Jazireeyan, I., Alizadeh, M., Pirooznia, M., Flury, J., Schuh, H., & Soja, B. (2023). Analyzing the Ionospheric Irregularities Caused by the September 2017 Geomagnetic Storm Using Ground-Based GNSS, Swarm, and FORMOSAT-3/COSMIC Data near the Equatorial Ionization Anomaly in East Africa. Remote Sensing, 15(24), 5762. https://doi.org/10.3390/rs15245762

[15] Webb, W. L. (1972). Thermospheric circulation. MIT Press (MA).

[16] Berényi, K. A., Heilig, B., Urbá', J., Kouba, D., Kis, Á., & Barta, V. (2023). Comprehensive analysis of the ionospheric response to the largest geomagnetic storms from solar cycle 24 over Europe. Frontiers in Astronomy and Space Sciences, 10. https://doi.org/10.3389/fspas.2023.1092850

[17] Astafyeva, E., Zakharenkova, I., & Förster, M. (2015). Ionospheric response to the 2015 St. Patrick's Day storm: Global GPS observations. *Journal of Geophysical Research: Space Physics*, 120(10), 9023-9035. https://doi.org/10.1002/2015JA021629

[18] Borries, C., Berdermann, J., Jakowski, N., & Wilken, V. (2015). Ionospheric storms-A challenge for empirical forecast of the total electron content. Journal of Geophysical Research Space Physics, 120(4), 3175-3186. https://doi.org/10.1002/2015ja020988

[19] Cherniak, I., Zakharenkova, I., & Redmon, R. J. (2015). Dynamics of the high-latitude ionospheric irregularities during the 17 March 2015 St. Patrick's Day storm: Ground-based GPS measurements. Space Weather, 13(9), 585-597. https://doi.org/10.1002/2015sw001237

[20] Fejer, B. G., Jensen, J. W., & Su, S. Y. (2008). Quiet time equatorial F region vertical plasma drift model derived from ROCSAT-1 observations. *Journal of Geophysical Research: Space Physics*, 113(A5). https://doi.org/10.1029/2007JA012801

[21] Foster, J. C., Erickson, P. J., Coster, A. J., Goldstein, J., & Rich, F. J. (2002). Ionospheric signatures of plasmaspheric tails. *Geophysical Research Letters*, 29(13), 1623. https://doi.org/10.1029/2002GL015067

[22] Chali Idosa Uga. (2022). Effects of Geomagnetic Storm on Ionospheric TEC Variability over High Latitude Regions. International Journal of Astrophysics and Space Science, 10(2), 18-27. https://doi.org/10.11648/j.ijass.20221002.11

[23] Liu, J., Zhao, B., & Liu, L. (2010). Time delay and duration of ionospheric total electron content responses to geomagnetic disturbances. Annales Geophysicae, 28, 795-805. https://doi.org/10.5194/ANGEO-28-795-2010

[24] Li, W., Zhao, D., He, C., Shen, Y., Hancock, C. M., & Zhang, K. (2022). Strong Storm-effect behaviors of topside and bottom-side ionosphere under low solar activity: Case study in the geomagnetic storm during 25-27 August 2018. Authorea Preprints. https://doi.org/10.1002/essoar.10511115.1

[25] Hernández-Pajares, M., Juan, J. M., Sanz, J., Aragón-Ángel, A., García-Rigo, A., Salazar, D., & Escudero, M. (2009). The IGS VTEC maps: A reliable source of ionospheric information since 1998. Journal of Geodesy, 83(3-4), 263-275. https://doi.org/10.1007/s00190-008-0266-1

[26] Liu, Y. D., Zhao, X., Hu, H., Vourlidas, A., & Zhu, B. (2019). A comparative study of 2017 July and 2012 July Complex eruptions: Are solar superstorms Perfect storms in nature The Astrophysical Journal Supplement Series, 241(2), 15. https://doi.org/10.3847/1538-4365/ab0649